Comparative Study of AlGaN/GaN HEMTs with LPCVD- and PECVD-SiN_x Passivation

Xinhua Wang, Sen Huang, Yingkui Zheng, Ke Wei, Xiaojuan Chen, Guoguo Liu, Tingting Yuan, Weijun Luo, Lei Pang, Haojie Jiang, Hushan Cui, Junfeng Li, Chao Zhao and Xinyu Liu

Institute of Microelectronics, Chinese Academy of Sciences, Beijing 100029, China
E-mail: xyliu@ime.ac.cn, wangxinhua@ime.ac.cn, huangsen@ime.ac.cn, Tel.: 86-10-82995595

Keywords: AlGaN/GaN HEMTs, current collapse, passivation, LPCVD, PECVD, SiN_x.

Abstract

Low-Pressure Chemical Vapor Deposition (LPCVD) technique is utilized for growth of SiN_x for passivation of AlGaN/GaN HEMTs. Compared with conventional PECVD-SiN_x passivation, effective current collapse suppression and remarkably improved RF power performance are achieved by LPCVD-SiN_x passivation. TEM-EDS mapping analysis suggests that the improved passivation from LPCVD-SiN_x is due to the reduced oxidation of the AlGaN barrier surface for HEMT devices in comparison to PECVD-SiN_x passivation. The strategy of "passivation-prior-to-ohmic" with LPCVD-SiN_x has shown improved performance for AlGaN/GaN HEMTs.

INTRODUCTION

AlGaN/GaN high-electron-mobility transistors (HEMTs) have enjoyed great success as the key components in RF/microwave power amplifiers and high-voltage power switches, primarily owing to the polarization-induced high mobility and high density 2-D electron gases (2DEG) at AlGaN/GaN hetero-interface and high breakdown *E*-field of (Al)GaN [1]. However, the high-electrical-conductivity 2DEG channel is generally at a short distance (e.g., ~20 nm) from the polarized AlGaN barrier surface, and could be easily affected by the depletion effect of surface traps. The slow detrapping behavior of the deep states would result in severe current collapse in GaN-based power amplifiers and power switches [2, 3].

To suppress the current collapse, plasma-enhanced chemical-vapor-deposited SiN_x layer is commonly adopted to passivate the surface states, except for the recently developed AlN passivation featuring polarization-charge-compensation concept [4]. There are several challenging issues for PECVD-SiN_x passivation, including: 1) relatively low film quality due to low growth temperature (typically below 350 ºC); 2) inescapable plasma-induced damages to (Al)GaN surface; and 3) long-term reliability induced by moisture erosion due to its loose texture [5]. In these regards, low-pressure chemical vapor deposition becomes an attractive technique for the growth of high quality SiN_x passivation layer for AlGaN/GaN HEMTs by virtue of its higher growth temperature (typically at above 600 ºC), non-plasma-activated sources, and moreover, compact film quality of LPCVD-SiN_x with less N-H and N-O bonds [6, 7]. Because the higher quality LPCVD-SiN_x film can now withstand the high thermal stress from the ohmic rapid thermal annealing step, this allows the device fabrication flow to take advantage of the more attractive "passivation-prior-to-ohmic" strategy. In addition, since LPCVD is an already mature technology in CMOS fabs, this approach is very attractive for mass production of AlGaN/GaN HEMTs because it can take advantage of the existing capability in CMOS line to further reduce fabrication cost.

Recently, LPCVD-SiN_x films have been implemented as gate dielectrics, as well as, passivation layer in CMOS-compatible process for GaN-based MIS-HEMTs on Silicon [8, 9]. Low leakage and low current collapse were realized simultaneously [10]. In this work, a standard CMOS LPCVD-SiN_x layer is successfully demonstrated for the passivation of AlGaN/GaN HEMTs. In comparison to conventional PECVD-SiN_x passivation, improved current collapse suppression and improved RF power performance has been achieved. The enhanced performance of LPCVD-SiN_x passivation has been demonstrated by this comparison study of the two AlGaN/passivation interfaces (LPCVD and PECVD).

9

DEVICE STRUCTURE AND FABRICATION

The AlGaN/GaN heterostructure used in this work consists of a 24-nm undoped $Al_{0.2}Ga_{0.8}N$ barrier, a 1-nm AlN interface enhancement layer, and a composite $Al_{0.02}Ga_{0.98}N$ /GaN (0.8 µm/0.8 µm) buffer layer. A 120-nm LPCVD-SiN_x passivation layer was deposited on the fresh epi layer at 780 °C and a low pressure of 300 mTorr after a standard RCA cleaning process. After dry etching openings of the LPCVD-SiN_x layer, ohmic contacts were formed with a Ti/Al/Ni/Au metal stack annealed at 850 °C for 50 s in ambient N_2. The contact resistance is measured to be 0.85

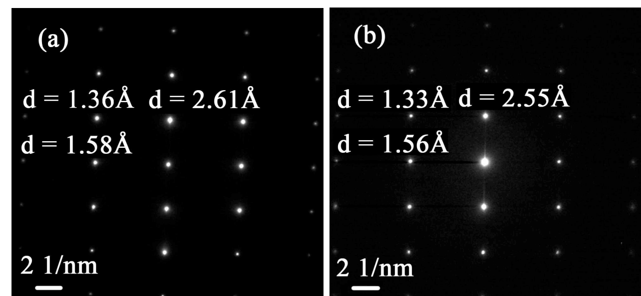

Fig. 1. X-ray diffraction pattern of (a) PECVD-SiN_x and (b) LPCVD-SiN_x. "d" is the interplanar spacing.

Ω • mm using transfer length method. Then boron ion implantation was used for device isolation. T-shape Ni/Au gate electrode is fabricated after gate opening, followed by a post-gate annealing at 350 °C for 5 min. For the reference PECVD-SiN_x-passivated AlGaN/GaN HEMTs, RCA wet cleaning was conducted on the fresh epi layer. However, the PECVD-SiN_x passivation was performed after ohmic contact formation, since the 120-nm low-temperature-grown PECVD-SiN_x (~300 °C) will crack from rapid thermal annealing process for ohmic metal. Note that an extra wet cleaning of the sample in a diluted NH_4OH solution and a 1-min *in-situ* N_2 plasma pretreatment were adopted before PECVD-SiN_x deposition. The followed fabrication process is similar to that of the LPCVSD-SiN_x-passivated AlGaN/GaN HEMTs. The gate length (L_G), gate-to-drain distance (L_{GD}), gate-to-source distance (L_{GS}), and gate width (W_G) of the fabricated HEMTs are 1, 2.75, 1.5 and 2×50 μm, respectively.

The refractive index of the LPCVD-SiN_x and PECVD-SiN_x passivation layer are measured to be 2.0 and 1.95, respectively. In addition, the interplanar spacings of the LPCVD-SiN_x passivation layer are smaller than the counterparts of the PECVD-SiN_x, as determined by X-ray diffraction technique equipped in TEM measurement system (Fig. 1). Both results suggest the standard-CMOS LPCVD-SiN_x features a more compact structure than conventional PECVD-SiN_x passivation, which provides better protection of the passivation/(Al)GaN interface from being oxidized, by H_2O or oxygen.

RESULTS AND DISCUSSION

Transfer characteristics of both LPCVD-SiN_x and PECVD-SiN_x passivated AlGaN/GaN HEMTs are compared and shown in Fig. 2(a). The LPCVD-SiN_x passivated sample shows higher peak drain current density and higher peak extrinsic transconductance than the PECVD-SiN_x passivated

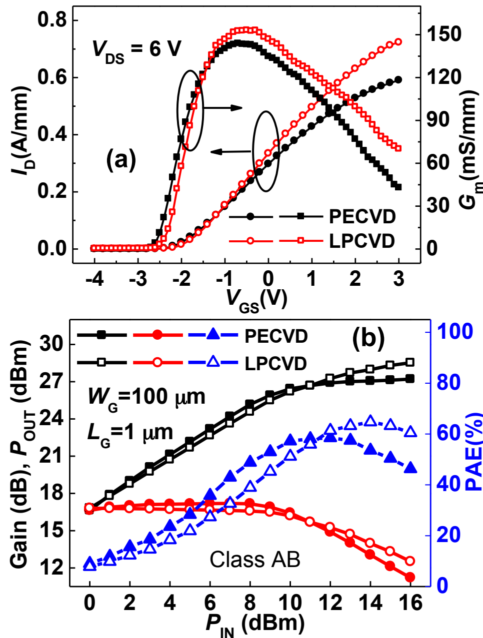

Fig. 2. (a) Transfer characteristics and (b) RF power performance of PECVD-SiN_x and LPCVD-SiN_x passivated AlGaN/GaN HEMTs measured at 4 GHz.

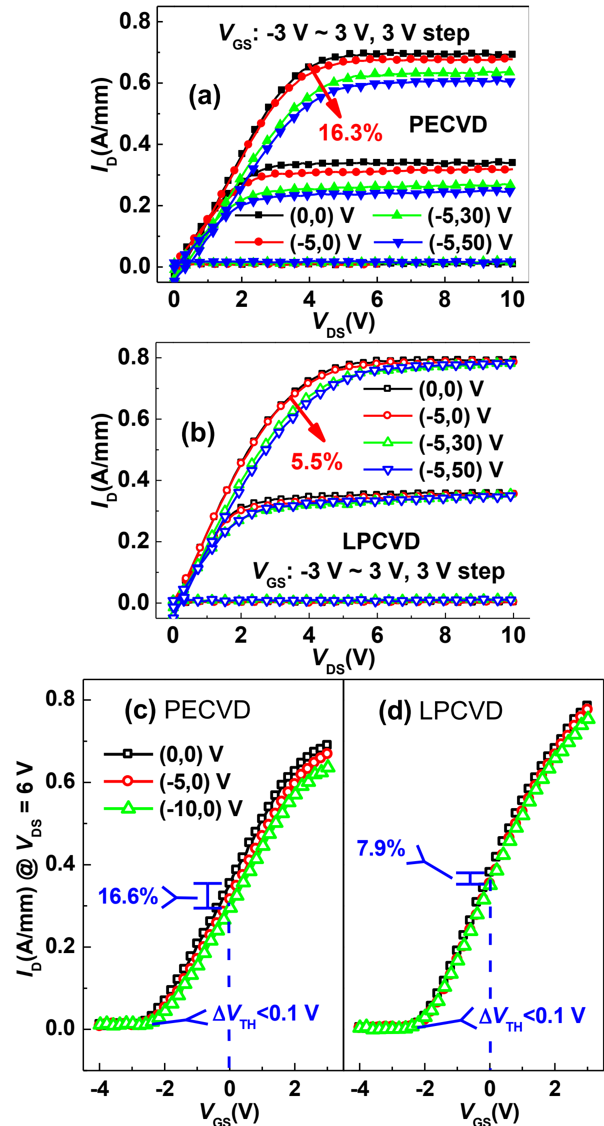

Fig. 3. Pulsed I_D-V_{DS} and I_D-V_{GS} characteristics of (a)/(c) PECVD-SiN_x and (b)/(d) LPCVD-SiN_x passivated AlGaN/GaN HEMTs, measured at different quiescent bias: (V_{GS}, V_{DS}) . The pulse width and period are 1 μs and 1 ms, respectively.

sample, although with similar threshold voltage (V_{TH} ~ -2 V). Moreover, the output power at 3 dB compression point and associated PAE of the LPCVD-SiN_x passivated samples, measured at 4 GHz with V_{DS} = 30 V, are 6.8 W/mm and 63.2%, respectively, which are 1.8 W/mm and 9.6% higher than that of the PECVD-SiN_x passivated ones (Fig. 2(b)).

The effectiveness of LPCVD-SiN_x passivation is also verified by pulse *I-V* characterization, as shown in Fig. 3. The pulse width and period were 1 μs and 1 ms, respectively. The collapse ratio was calculated using the expression of [1-$I_D(V_{GS}, V_{DS})/I_D(0,0)$], where $I_D(V_{GS},V_{DS})$ is measured after pulsed from the quiescent bias: (V_{GS},V_{DS}). Compared with the PECVD-SiN_x-passivated HEMTs, the collapse ratio of the LPCVD-SiN_x-passivated ones is much smaller at a high

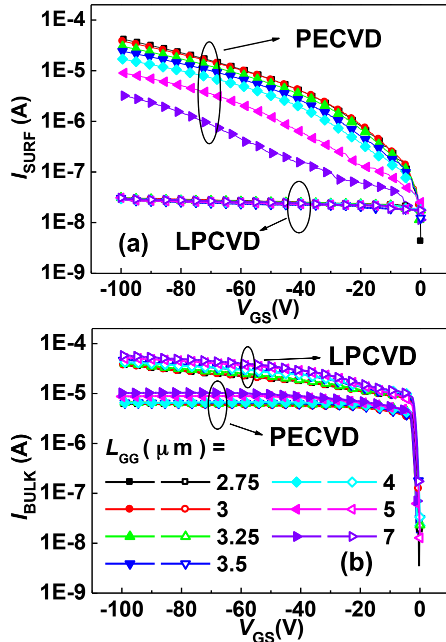

Fig. 4. (a) I_{SURF}-V_{GS} and (b) I_{BULK}-V_{GS} characteristics of PECVD-SiN_x and LPCVD-SiN_x passivated samples with various L_{GG}.

quiescent bias of (-5 V, 50 V), whether in the linear or saturation region (Fig. 3(a) and (b)). On the other hand, both samples exhibit slight threshold voltage shift (< 0.1 V) in pulsed transfer characterizations, as shown in Fig. 3(c) and (d). It suggests that surface-related traps are the dominant cause for the current collapse [11].

Double gate structures with gate-to-gate distance (L_{GG}) ranging from 2.75 to 5 μm, is introduced to distinguish lateral surface leakage current (I_{SURF}) via SiN_x/AlGaN interface from vertical leakage current (I_{BULK}). The I_{SURF} in the PECVD-SiN_x-passivated HEMTs increases as L_{GG} decreases, while that in the LPCVD-SiN_x passivated ones is much lower and remains constant for all the L_{GG} (Fig. 4(a)). Two-Dimensional Variable Range Hopping (2D-VRH) assisted by high-density interface states is considered as a possible cause for I_{SURF} [12], which indicates that the traps at LPCVD-SiN_x/AlGaN interface are less than that of PECVD-SiN_x. The higher I_{BULK} in the LPCVD-SiN_x passivated HEMTs further confirms the effective mitigation of 'virtual gate' formed by interface traps (Fig. 4(b)) [2], which will enhances the peak *E*-field on drain side of the gate edge and results in higher gate tunneling current. The relation between the reduction/increase in I_{SURF} and the subsequent mitigation/degradation of current collapse agrees well with the conclusion in other works [13, 14].

TEM-EDS mapping of the SiN_x/AlGaN interface is performed to investigate the source of interface traps, as shown in Fig. 5. The intensity of element signals is slightly adjusted to obtain good contrast, but it would not affect the comparison. The LPCVD-SiN_x passivated HEMTs exhibit narrower oxygen-contaminated region (~2 nm) than that of the PECVD-SiN_x passivated interface (~6 nm). Oxygen-related bonds such as Ga-O are confirmed to be the source of surface traps in AlGaN/GaN HEMTs [15]. The oxidation of

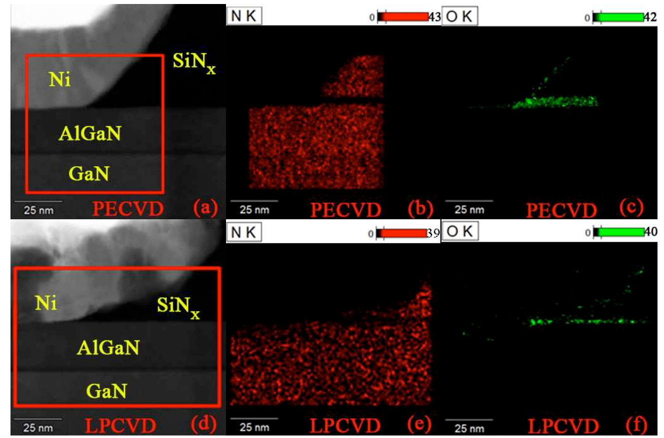

Fig. 5. Element distribution of SiN_x/AlGaN interfaces analyzed by TEM-EDS mapping (in red pane). PECVD/LPCVD: (a)/(d) cross-sectional view, (b)/(e) nitrogen, (c)/(f) oxygen

the AlGaN barrier surface in both samples is usually due to the exposure of AlGaN surface to oxygen-containing environment during the fabrication process, particularly, the ohmic annealing at above 800 ºC. Therefore, the strategy of 'passivation-prior-to-ohmic' is highly desirable in fabrication of AlGaN/GaN HEMTs, just as the LPCVD-SiN_x passivated ones. The thin oxidation layer in the LPCVD-SiN_x passivated samples is due to the air exposure between RCA cleaning and LPCVD-SiN_x passivation, which gives rise to the residual current collapse in the LPCVD-SiN_x passivated HEMTs[15].

CONCLUSIONS

Standard-CMOS LPCVD-SiN_x is utilized for passivation of AlGaN/GaN HEMTs. Effective current collapse suppression and RF power performance improvement are achieved. The strategy of "passivation-prior-to-ohmic" with LPCVD-SiN_x has shown improved performance for AlGaN/GaN HEMTs.

ACKNOWLEDGEMENTS

This work was supported by the National Science and Technology Major Project of the Ministry of Science and Technology of China under Grant 2014ZX01002101, and the National Natural Science Foundation of China under Grant 61404163 and 61474138.

REFERENCES

[1] Y. F. Wu, A. Saxler, M. Moore, R. P. Smith, S. Sheppard, P. M. Chavarkar, T. Wisleder, U. K. Mishra, and P. Parikh, "30-W/mm GaNHEMTs by field plate optimization," *IEEE Electron Device Lett.,* vol. 25, no. 3, pp. 117-119, Mar. 2004.
[2] G. Koley, V. Tilak, L. F. Eastman, and M. G. Spencer, "Slow transients observed in AlGaN/GaN HFETs: effects of SiN/sub x/ passivation and UV illumination," *IEEE Trans. Electron Devices,* vol. 50, no. 4, pp. 886-893, Apr. 2003.
[3] S. Huang, Q. Jiang, Jiang, S. Yang, C. Zhou, and K. J. Chen, "Effective Passivation of AlGaN/GaN HEMTs by ALD-Grown AlN Thin Film," *IEEE Electron Device Lett.,* vol. 33, no. 4, pp. 516-518, 2012.
[4] K. J. Chen and S. Huang, "AlN passivation by plasma-enhanced atomic layer deposition for GaN-based power switches and power amplifiers," *Semicond.Sci.Technol.,* vol. 28, no. 7, p. 074015, Jul. 2013.

9

[5] Feng Gao, C. V. Thompson, J. d. Alamo, and T. Palacios, "Electrochemical Degradation Mechanisms in AlGaN-GaN HEMTs," in *CS MANTECH Conference*, Denver, USA 2014, pp. 29-32.
[6] J. Yota, J. Hander, and A. A. Saleh, "A comparative study on inductively-coupled plasma high-density plasma, plasma-enhanced, and low pressure chemical vapor deposition silicon nitride films," *J. Vac. Sci. Technol. A,* vol. 18, no. 2, pp. 372-376, Oct. 2000.
[7] T. Oku, M. Okumura, M. Totsuka, T. Shiga, and M. Takemi, "Moisture resistance of insulating films for compound semiconductor devices," in *CS MANTECH Conference*, Denver, USA 2014, pp. 179-182.
[8] M. Van Hove, S. Boulay, S. R. Bahl, S. Stoffels, K. Xuanwu, D. Wellekens, K. Geens, A. Delabie, and S. Decoutere, "CMOS Process-Compatible High-Power Low-Leakage AlGaN/GaN MISHEMT on Silicon," *IEEE Electron Device Lett.,* vol. 33, no. 5, pp. 667-669, 2012.
[9] B. De Jaeger, M. Van Hove, D. Wellekens, X. Kang, H. Liang, G. Mannaert, K. Geens, and S. Decoutere, "Au-free CMOS-compatible AlGaN/GaN HEMT processing on 200 mm Si substrates," in *24th International Symposium on Power Semiconductor Devices and ICs (ISPSD)* 2012, pp. 49-52.
[10] S.-W. Moon, J. Lee, D. Seo, S. Jung, H. G. Choi, H. Shim, J. S. Yim, J. Twynam, and S. D. Roh, "High-voltage GaN-on-Si hetero-junction FETs with reduced leakage and current collapse effects using SiN x surface passivation layer deposited by low pressure CVD," *Jpn. J. Appl. Phys.,* vol. 53, p. 08NH02, Jul. 2014.
[11] G. Meneghesso, F. Zanon, M. J. Uren, and E. Zanoni, "Anomalous Kink Effect in GaN High Electron Mobility Transistors," *IEEE Electron Device Lett.,* vol. 30, no. 2, pp. 100-102, Feb. 2009.
[12] J. Kotani, M. Tajima, S. Kasai, and T. Hashizume, "Mechanism of surface conduction in the vicinity of Schottky gates on AlGaN/GaN heterostructures," *Appl. Phys. Lett.,* vol. 91, no. 9, pp. 093501-093503, Aug. 2007.
[13] W. S. Tan, M. J. Uren, P. A. Houston, R. T. Green, R. S. Balmer, and T. Martin, "Surface leakage currents in SiNx passivated AlGaN/GaN HFETs," *IEEE Electron Device Lett.,* vol. 27, no. 1, pp. 1-3, Jan. 2006.
[14] Z. Tang, S. Huang, X. Tang, B. Li, and K. J. Chen, "Influence of AlN Passivation on Dynamic ON-Resistance and Electric Field Distribution in High-Voltage AlGaNGaN-on-Si HEMTs," *IEEE Trans. Electron Devices,* vol. 61, no. 8, pp. 2785-2792, Aug. 2014.
[15] S. Yang, Z. Tang, K.-Y. Wong, Y.-S. Lin, Y. Lu, S. Huang, and K. J. Chen, "Mapping of interface traps in high-performance Al2O3/AlGaN/GaN MIS-heterostructures using frequency- and temperature-dependent C-V techniques," in *2013 IEEE International Electron Devices Meeting* 2013, pp. 6.3.1-6.3.4.

ACRONYMS

LPCVD: Low-Pressure Chemical Vapor Deposition
PECVD: Plasma-Enhanced Chemical Vapor Deposition
CMOS: Complementary Metal-Oxide-Semiconductor Transistor
HEMT: High-Electron-Mobility Transistor
TEM: Transmission Electron Microscope
EDS: Energy Dispersive Spectrometer
PAE: Power-Added Efficiency
2D-VRH: Two-Dimensional Variable Range Hopping